Compressed Sensing Undersampled MRI Reconstruction using Iterative Shrinkage Thresholding based on NSST

Min Yuan, BingxinYang, Yide Ma*, Jiuwen Zhang, Runpu Zhang, and Kun Zhan
School of Information Science & Engineering
Lanzhou University
Lanzhou, China

***Abstract*—Compressed sensing (CS) has great potential for use in reducing data acquisition time in MRI. Generally sparsity is used as a prior knowledge to improve the quality of reconstructed image. In this paper, we propose an effective compressed sensing rapid MR imaging method incorporating Non-Subsampled Shearlet transform (NSST) sparsity prior information for MR image reconstruction from highly undersampled k-space data. In particular, we have implemented the more flexible decomposition with 2n directional subbands at each scale using NSST to obtain the prominent sparser representation for MR images. In addition, the mixed L1-L2 norm of the coefficients from the prior component and residual component is used to enforce joint sparsity. Numerical experiments demonstrate that the proposed method can significantly increase signal sparsity and improve the ill-conditioning of MR imaging system using NSST sparsity regularization. The evaluations on a T2-weighted brain image and a MR phantom experiment demonstrate superior performance of the proposed method in terms of reconstruction error reduction, detail preservation and aliasing, Gibbs ringing artifacts suppression compared to state-of-the-art technique. Its performance in objective evaluation indices outperforms conventional CS-MRI methods prominently.**

***Index Terms*—Compressed sensing (CS), magnetic resonance imaging (MRI), Non-Subsampled Shearlet transform (NSST), iterative soft thresholding (IST)**

I. INTRODUCTION

Magnetic Resonance Imaging (MRI), is a widely used non-invasive imaging modality for clinical diagnosis. However, MRI relatively slow imaging speed remains a great challenge for clinical application. An effective way to speed up MR imaging is *k*-space undersampling. However, undersampling violates the Nyquist sampling criterion, resulting in aliasing artifacts, inadequate image resolution and excessive Gibbs ringing artifacts.

Compressed Sensing (CS)[1][2] is a brandnew signal acquisition and compression theory. As a promising method, CS[3] has been introduced to MR image reconstruction, so-called compressed sensing MRI (CS-MRI)[4]-[6]. CS-MRI allows high quality reconstruction from undersampled *k*-space data by solving a constrained minimization problem using nonlinear optimization algorithm by enforcing the sparsity of images in a certain predefined sparsifying transform, such as the traditional 2D separable wavelet transform[4], Total variation(TV)[4][7][8], Contourlet[9][10], Sharp Frequency Localization Contourlet (SFLCT)[11][12], dual-tree complex wavelet transform (DT-CWT)[13][14], complex double-density dual-tree DWT[15]. The The structured sparsity such as Gaussian scale mixture (GSM) model [16][17]and wavelet tree sparsity[18][19] for exploiting the dependencies between wavelet coefficients have been introduced to CS-MRI reconstruction. In terms of the Restricted Isometry Property (RIP) condition in CS, incorporating a prior knowledge to enhance the sparsity into the reconstruction can reduce the reconstruction error and improve the reconstruction of details effectively. In the past several years these analytical sparsifying transforms have been successfully applied to CS-MRI and demonstrate high quality reconstructions from undersampled data. Some of these transforms have been combined to further improve the reconstruction [20]-[23]. Dictionary learning enables adaptive sparser representation of MR images than the general sparsifying transforms, which has been applied in CS-MRI [24].

The quality of reconstructed images largely depends on the performance of exploiting the sparsifying prior in CS-MRI, which are key to accurate CS reconstruction. Therefore an outstanding sparsifying transform suitable for representing MR images should be adopted as sparsity prior in CS-MRI reconstruction. The motivation of our study comes from the morphology that MR images consist of different components in various orientations, which cannot be sparsely represented by existing sparse representation sufficiently and yet dictionary learning is at the expense of sacrificing time. In this paper we proposed a novel CS-MRI image reconstruction method from highly undersampled *k*-space data to improve the quality of reconstructed MR images by enhancing the sparsity in Non-Subsampled Shearlet transform (NSST) domain. With the ability to capture intrinsic geometrical features of multidimensional data efficiently and sparsely represent images containing edges optimally, the prominent sparse representation-NSST is adopted as prior knowledge for the regularization in CS-MRI. The numerical computation employs a corresponding iterative NSST thresholding algorithm to solve this optimization inverse problem.

* Corresponding author. Email: yidema@gmail.com

978-1-4799-5274-8/14/$31.00 ©2014 IEEE

II. BACKGROUND

A. Problem Formulation

The common model of data acquisition with incomplete measurements for CS-MRI is given by the following formulation:

$$\mathbf{y} = \mathbf{F_u x} + \mathbf{n} \tag{1}$$

where $\mathbf{x} \in \mathbb{C}^N$ is the reconstructed image, $\mathbf{y} \in \mathbb{C}^M$ is the acquired *k*-space measurement data corrupted with the noise n, and F_u is the undersampled Fourier transform operator which directly relies on the *k*-space undersampling scheme. Suppose that $\mathbf{x}$ is represented as $\mathbf{x} = \mathbf{\Psi\alpha}$, where $\mathbf{\Psi}$ represents the sparsity prior associated with the transform under which MR image $\mathbf{x}$ has a sparse representation or approximation. Then the measured data is given by $\mathbf{y} = \mathbf{F_u \Psi \alpha} + \mathbf{n}$, where $\mathbf{F_u \Psi}$ represents the sensing matrix.

According to CS theory, CS-MRI claims to reconstruct MR image from undersampled *k*-space data by enforcing the image sparsity [4]. That is $\mathbf{x}$ can be accurately reconstructed from a small subset of *k*-space data by solving the following ℓ_0 norm minimization problem.

$$\min_{\alpha} \|\boldsymbol{\alpha}\|_0 \quad s.t. \quad \mathbf{y} = \mathbf{F_u \psi \alpha} \tag{2}$$

However, the ℓ_0 norm is not convex and the computational complexity of the optimization is NP-hard [7]. It has been proved that under certain condition, ℓ_0 norm problem is equivalent to ℓ_1 norm. Thus the reconstruction can be obtained by solving the following constrained convex optimization:

$$\min_{\alpha} \|\boldsymbol{\alpha}\|_1 \quad s.t. \quad \|\mathbf{y} - \mathbf{F_u \psi \alpha}\|_2 < \varepsilon \tag{3}$$

where ε is a statistic describing the magnitude of the error, that defined as the noise variance or the maximum allowable error in the approximation. Minimizing the objective function $\|\boldsymbol{\alpha}\|_1$ promotes the sparsity of the images. The constraint $\|\mathbf{y} - \mathbf{F_u \psi \alpha}\|_2 < \varepsilon$ enforces the fidelity of the reconstruction to the measured *k*-space data. Besides, constrained ℓ_1 norm convex optimization problem in Eq. (3) can be written in unconstrained Lagrangian form

$$\min_{\alpha} \frac{1}{2} \|\mathbf{y} - \mathbf{F_u \psi \alpha}\|_2^2 + \lambda \|\boldsymbol{\alpha}\|_1 \tag{4}$$

The second term of Eq. (4) is a regularization term that represents a prior sparse information of original images. λ is a regularization parameter governing the tradeoff between the data fidelity and its sparsity.

B. Non-Subsampled Shearlet transform

The shearlet transform, introduced by the authors and their collaborators in [25] and [26], is a very recent sibling in the family of geometric image representations. The shearlet representation originally derived from the framework of affine systems with composite dilations [25]-[27]. The shearlet frame elements associated to shearlet transform are defined at various scales. The shearlet transform is a multiscale directional transform which is especially adapted to localize distributed discontinuities such as edges. Unlike conventional multiresolution analysis tool, shearlet representation is theoretically optimal in representing directional and anisotropic features in images, and has the ability to accurately and efficiently capture the geometric information of multidimensional data at various scales. Consequently, NSST is an awesome choice for CS-MRI as sparsity prior constrain in the regularization. Incorporating the shearlet sparsifying prior knowledge into the process of image reconstruction, we can get the sparse NSST coefficients and then get the reconstructed MR images by solving fore-mentioned constrained optimization problem. Refer to [25]-[28] for more details about the mathematical framework and the implement of discrete shearlet transform.

III. PROPOSED METHOD

On account of existing different defects in fore-mentioned sparsifying transforms, such as lack of shift invariance, which could easily produce pseudo-Gibbs artifacts around the singularities, decomposed directional subbands only at 2^n directions in terms of directional selectivity, they may not provide sufficient sparse representation for sharp spatial gradients and intrinsic geometrical features contained in MR images. To overcome these limitations, on account of the MR images consist of curve singularities and anisotropic directional features, a more appropriate sparsifying prior with highly directional sensitivity and anisotropy should be applied to reconstruction. So we employ a special form of shearlet transform-------NSST as sparsifying prior in CS-MRI reconstruction.

A. NSST sparsity prior

- **exhibit optimal sparsity and optimal approximation property**

The shearlet elements form a tight frame of well-localized waveforms, at various scales and directions, and are optimally sparse in representing images with edges. This property is very important for MRI reconstruction in a CS application because it results in MR images that are more compressible and hence more effective to be reconstructed. We can achieve better approximation performance and better sparse representation by shearlet coefficients compared to others.

- **exhibit highly directional sensitivity and anisotropy**

Unlike the isotropic elements of wavelet bases, a pair of trapezoid elements of shearlet transform possesses very high directional sensitivity and anisotropy. Such elements are very efficient in representing curve-like edges and texture features. Contourlet and SFLCT can capture the geometry of images only in 2^n directions which is not optimal for MR images, because the feature information of organ, tissue or blood vessel could be in all directions. It worth being noted that an outstanding advantage of shearlet transform is that there are no restrictions on the number of directions for the shearing compared with other 'directional wavelets'. The flexibility of directional decomposition cannot achieve for a fan filter implementation of the DFBs.

Considering the problems of aliasing and shift-variant caused by decimating, in our implementation for CS-MRI, we adopt the particular form implementation of the time-domain based shearlet transform. This will be simply referred to as the Non-Subsampled Shearlet Transform (NSST), which is to use the non-subsampled Laplacian pyramid (LP) transform with several different combinations of the shearing filters. As a consequence, NSST exhibits excellent shift invariance. The main advantages are that the shearing filter can have smaller support sizes than the directional filters used in the contourlet transform and can be implemented much more efficiently.

Note that the only one restriction on the shearing filters is that the size of the filter should be more than or equal to the maximum number of directional subbands. In the experiment, considering the accuracy we have implemented the decomposition with $2\times n$ directional subbands at each scale using NSST, which is more flexible than 2^n directions of SFLCT. Thus it benefits to capture the intrinsic characteristics information of MR images at more different directions using NSST. Therefore, it only needs less transform domain coefficients than the other sparsifying transforms when the curve characteristics of MRI are expressed using NSST. In this implementation, we have a large flexibility in the choice of the number of orientations for decomposition. In practice, we use a Meyer wavelet window to construct the directional shearing filters. The shearing filters of sizes 12×12, 12×12, 12×12 from finer to coarser were used with the number of shearing directions chosen to be 12, 12, and 12. NSST (12, 12, 12) indicates that a Meyer-based shearing filter of size 12 with 12 directions was applied to the first, second and third decomposition level.

B. Compressed Sensing MRI using Iterative Shrinkage Thresholding based on NSST

The reconstruction problem from undersampling *k*-space data actually belongs to an underdetermined system of linear equations. It is the good way for improving performance to incorporate a sparse prior knowledge into the nonlinear reconstruction. The proposed approach in this paper is based on NSST as the representation of sparse prior for CS-MRI.

Different numerical reconstruction algorithms to solve Eq. (5) optimization problem [29]-[35] have been proposed in the past few decades. Among the existing algorithms, the iterative shrinkage thresholding algorithm (ISTA) is straightforward, often-used and effective for solving of linear inverse problems. The reason is that ISTA with good robustness is easy to implement and can be integrated easily with existing sparsifying transforms in practical application. These properties are significant for CS-MRI. Considering the effectiveness and the convenience of ISTA, we adopt improved iterative shearlet thresholding to solve CS-MRI.

The interpretation and convergence of iterative thresholding algorithm for solving constraint ℓ_1 norm optimization were discussed in the literatures [29][31]. The core idea of iterative thresholding is the objective function is guaranteed to decrease on each iteration of the algorithm. This algorithm iteratively performs a soft thresholding to decrease the ℓ_1 norm of the coefficients α and a gradient descent to decrease the value of $\|\mathbf{y} - \mathbf{F_u}\boldsymbol{\psi}\boldsymbol{\alpha}\|_2$. Eq. (4) can be simply solved by iterative shearlet thresholding:

$$\begin{aligned}\boldsymbol{\alpha}_{\mathbf{k+1}} &= S_{\theta_k}\left(\frac{1}{c}(\mathbf{F_u}\boldsymbol{\psi})^*(\mathbf{y} - \mathbf{F_u}\boldsymbol{\psi}\boldsymbol{\alpha}_{\mathbf{k}}) + \boldsymbol{\alpha}_{\mathbf{k}}\right) \\ &= S_{\theta_k}\left(\frac{1}{c}(\mathbf{F_u}\boldsymbol{\psi})^*\mathbf{r} + \boldsymbol{\alpha}_{\mathbf{k}}\right)\end{aligned} \tag{5}$$

Where $(\mathbf{F_u}\boldsymbol{\psi})^*$ denotes the adjoint transpose operator of $\mathbf{F_u}\boldsymbol{\psi}$, $\boldsymbol{\psi}$ and $\boldsymbol{\psi}^*$ denote the shearlet inverse and forward transform, respectively. The choice of c should satisfy $c > \|(\mathbf{F_u}\boldsymbol{\psi})^*(\mathbf{F_u}\boldsymbol{\psi})\|_2 = \lambda_{\max}((\mathbf{F_u}\boldsymbol{\psi})^*(\mathbf{F_u}\boldsymbol{\psi}))$ (the maximal eigenvalue of the matrix $(\mathbf{F_u}\boldsymbol{\psi})^*(\mathbf{F_u}\boldsymbol{\psi})$). $\mathbf{r} = \mathbf{y} - \mathbf{F_u}\boldsymbol{\psi}\boldsymbol{\alpha}_{\mathbf{k}}$ is the residual in k-space. The thresholding function can be used in the coefficient iteration. Here $S_{\theta_k}(\boldsymbol{\alpha})$ is a soft thresholding operator to shrinkage each entry $\boldsymbol{\alpha}_{\mathbf{k}}$ of vector $\boldsymbol{\alpha}$ according to the following:

$$S_{\theta_k}(\boldsymbol{\alpha}_{\mathbf{k}}) = \begin{cases} 0 & , \textit{ if } |\boldsymbol{\alpha}_{\mathbf{k}}| \le \boldsymbol{\theta}_{\mathbf{k}} \\ \boldsymbol{\alpha}_{\mathbf{k}} - \dfrac{|\boldsymbol{\alpha}_{\mathbf{k}}|}{\boldsymbol{\alpha}_{\mathbf{k}}}\boldsymbol{\theta}_{\mathbf{k}} & , \textit{ otherwise} \end{cases} \tag{6}$$

Since $\boldsymbol{\alpha}$ is a complex vector for MR images, a complex thresholding operator should be defined. I. Daubechies [29] extended the definition of the operator and derived a complex thresholding operator,which is defined as $S_\theta(|\boldsymbol{\alpha}_{\mathbf{i}}|\mathbf{e}^{\mathbf{j}\omega}) = S_\theta(|\boldsymbol{\alpha}_{\mathbf{i}}|)\mathbf{e}^{\mathbf{j}\omega}$, $\omega \in [0, 2\pi)$.

In order to eliminate the effect of the magnitude of MR images on stop criteria, a relative error tolerance [12] $\eta = \|\mathbf{y} - \mathbf{F_u}\boldsymbol{\psi}\hat{\boldsymbol{\alpha}}\|_2 / \|\mathbf{y}\|_2$ is adopted to replace absolute stop criteria related to ε of Eq. (4). The decreasing factor ρ is adopted to decrease the threshold in each iteration. The computational parameters η and ρ in the algorithm are constants, and we set them to be the same in all the experiments. The selecting problem of the value of η and ρ were investigated in the paper [12]. From empirical analysis, $\eta = 10^{-6}$ and $\rho = 0.8$ are an appropriate choice to acquire good performance for CS-MRI. The improved CS-MRI reconstruction algorithm from undersampled k-space measurements using iterative NSST soft thresholding is summarized in Algorithm 1.

Algorithm 1. Algorithm to reconstruct MR image from undersampled *k*-space measurements using NSST_IST.

Inputs: NSST operator $\boldsymbol{\psi} \in \mathbb{C}^{n \times d}$, sensing matrix $\mathbf{A} = \mathbf{F_u}\boldsymbol{\psi}$, undersampled *k*-space data $\mathbf{y} \in \mathbb{C}^{m}$, relative error tolerance η and decreasing factor $\rho, (0 < \rho < 1)$

Output: solution of the optimization — the estimated coefficients $\hat{\boldsymbol{\alpha}}$, the reconstructed image $\hat{\mathbf{x}} = \boldsymbol{\psi}\boldsymbol{\alpha}_\mathbf{k}$

Initialization:

Threshold $\theta_0 = \max((\mathbf{F_u}\boldsymbol{\psi})^* \mathbf{r_0})$, Coefficient vector $\boldsymbol{\alpha}_\mathbf{0} = [(0, \ldots, 0)_{1 \times n}]^T$, the reconstructed image $\mathbf{x_0} = \boldsymbol{\psi}\boldsymbol{\alpha}_\mathbf{0}$, Residual $\mathbf{r_0} = \mathbf{y}$, Maximal iteration number $k_{\max}$

Iteration:

While relative residual $R_k = \|\mathbf{y} - \mathbf{F_u}\boldsymbol{\psi}\boldsymbol{\alpha}_k\|_2 / \|\mathbf{y}\|_2 \geq \eta$ and $k < k_{\max}$

1) Update coefficient vector according to soft threshold $\boldsymbol{\alpha}_\mathbf{k+1} = \boldsymbol{\alpha}_\mathbf{k} + S_{\theta_k}((\mathbf{F_u}\boldsymbol{\psi})^* \mathbf{r_k})$
2) Computer residual $\mathbf{r_{k+1}} = \mathbf{y} - \mathbf{F_u}\boldsymbol{\psi}\boldsymbol{\alpha}_\mathbf{k+1}$
3) Update the threshold $\boldsymbol{\theta}_\mathbf{k+1} = \rho\boldsymbol{\theta}_\mathbf{k}$

End Until the stop criteria is met.

IV. EXPERIMENTS

A. Framework

To evaluate the performance of the proposed approach, we performed a large number of experiments on a high resolution phantom and a representative human brain T2-weighted MR image. All the experiments were implemented using a laptop equipped with an Intel Core i5-2450M CPU at 2.50GHz and 6GB memory, employing a 32-bit Windows7 operating system. The routines were tested in Matlab R2011b. The CS data acquisition was simulated by undersampling the 2D discrete Fourier transform of MR images. Sampling schemes used in the experiments include 2D variable density random sampling and pseudo radial sampling. For these MR images, results and performance of proposed reconstruction method are compared with four classical or state-of-the-art schemes: zero-filling, TV-CG [4], Orthogonal Discrete Wavelet Transform (ODWT) [4] based, SFLCT [12] based CS-MRI reconstruction. For ODWT based method, images are decomposed using the 'db4' wavelet with 4 vanishing moments and four decomposition levels, denoted as ODWT. For implementing SFLCT method [12], the level of decomposition is set to 4. SFLCT is with decomposition level [5, 4, 4, 3], which means four decomposition levels and 2^5, 2^4, 2^4, 2^3 directional subbands from coarse to fine scales. The 'pkva' quincunx/fan filter is employed as a decomposition filter in SFLCT. For NSST based CS-MRI reconstruction, the level of decomposition, the size of shearing filters and the maximum number of directional subbands have been mentioned in Section III.

B. Results and Subjective Evalution

In general, the noiseless case can be solved by performing problem (3). We first study the noiseless scenario to see the performance of NSST based sparsity representation and its application in CS-MRI reconstruction.

1) Axial T2-weighted image of the brain

In Fig.1, variable density random sampling pattern with 12.5% undersampling factor is employed on an Axial T2-weighted image of the brain. Obviously, the reconstructed MRI images using other four methods suffer considerably from less contrast and less visibility in some tissue structures, which is clearly seen to have many undesirable artifacts and loss of features. TV-CG is unable to remove aliasing artifacts seen in the zero-filling result. On the other hand, as shown in Fig.1(g), the reconstruction using NSST-based approach relatively devoid of aliasing artifacts. Gibbs ringing artifacts have been drastically mitigated employing the proposed approach compared with the other four reconstructions due to NSST sparsity constraint in our method. The quality of reconstructed results has a large degree of improvement utilizing the proposed approach. Specifically, in comparison of other methods, the reconstructed images (g) using the proposed approach can provide good contrast between gray and white matter. The anatomic structure of bilateral basal ganglia was depicted well. Cerebral cisterns and sulci were present with clear border. The reconstructed MR images using NSST-based approach with higher contrast and spatial resolution can preserve integrity of boundary and texture of tissue perfectly. (h) ~ (l) in Fig.1 shows the magnitudes of the reconstruction error for five methods on the same scale. The reconstructed result using the proposed approach yields least error among these five algorithms. The magnitudes of the reconstruction error of comparing four methods show much

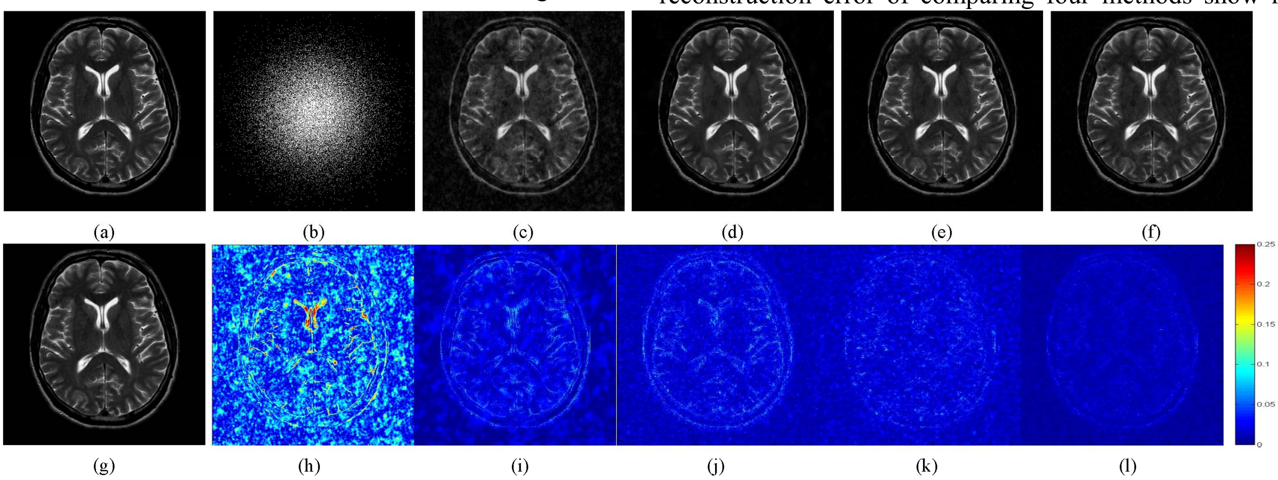

Fig.1. Comparison of NSST-based CS-MRI reconstruction versus other four scenarios from undersampled k-space using variable density random sampling pattern. (a) Axial T2-weighted reference image of the brain(512 × 512), (b) k-space sampling mask of variable density random sampling with 12.5% sampling rate, (c)~(g) Reconstruction by zero-filling, TV-CG, ODWT-based, SFLCT-based and NSST-based CS-MRI, respectively, (h)~(l) Comparison of magnitude of reconstruction error for five methods between (a) and (c)~(g) with the gray scale of [0,0.25].

more regions of high error indicating loss of structured features.

2) MR phantom

Fig.2 shows the case of a standard resolution MR phantom. The results show that the reconstructed image quality using zero filling and ODWT-based is rather poor. The corresponding figures with less contrast and loss of considerable details show the presence of artifacts. SFLCT-based reconstructed image quality has improved slightly, but which contains some Gibbs ringing artifacts and blurry boundaries.

Reconstructed phantom (g) of Fig.2 via the proposed method with improved visual quality looks much better compared to other four images. It is clear enough to permit the visualization of small details with less graininess. More details are visible because the resolution is higher as shown in Fig.2. The reconstruction result (a1) ~ (f1) of Fig.2 are enlargements of (a), (c) ~ (g) for a certain region. It's worth noting that, from (a1) ~ (f1), the reconstructed image by the proposed algorithm with the uniform background just like the original image eliminates artifacts to some extent. The reconstructed small comb and strip object nearby used to represent intrinsic features appear most clearly in Fig.2 (f1) by the proposed algorithm among five results, yet the comb is blurred into a mass so that the teeth of comb is unable to be distinguished in TV-CG reconstruction. But the boundary of square below the comb in Fig.2 (f1) is not as distinct as TV-CG reconstruction.

The above comparison demonstrates that NSST-based CS-MRI reconstruction approach is highly effective at preserving more important characteristics information and mitigating Gibbs ringing artifact. It can obviously improve the quality of reconstructed MR image which meets the requirements of clinical diagnostic applications, which outperforms methods based on ODWT, SFLCT and NSST as well as other existing ones.

C. Objective Evalution Indices

Besides the visual appearance, the objective criteria are also essential for the reconstructed Image Quality Assessment (IQA). In order to measure the performance of the algorithm fully, we need to evaluate reconstructions quality quantitatively or qualitatively. The quality of the reconstruction is quantified using six metrics—peak signal-to-noise ratio (PSNR), Structural SIMilarity (SSIM) index [35], relative ℓ_2 norm error (RLNE) [12] and transferred edge information (TEI) [36].

The curves (a) ~ (d) of Fig.3 show comparision of objective assessment indices PSNR, SSIM, RLNE and TEI versus undersampling rate, respectively, using zero-filling, TV-CG, ODWT-based, SFLCT-based CS-MRI reconstruction with comparison to the proposed NSST-based algorithm at different undersampling rates for a T2 weighted brain image with variable density random sampling mask. These assessment parameters demonstrate NSST-based CS-MRI reconstruction algorithm obtains the highest objective criteria except SSIM after a few iterations. This also demonstrates that the proposed algorithm can give the best reconstructed image at considerable low sampling rate in *k*-space measurements. The values of PSNR and TEI of NSST-based CS-MRI are the highest among comparing algorithms, while RLNE is the minimum. From Fig.3, it is obvious that the proposed algorithm not only can obtain minor reconstruction error, good edge-preserving characteristics but also can improve the spatial detail information and preserve the structural similarity of image than the existing algorithms (especially in the enlargements), which can also be justified by the obtained maximum values of evaluation indices. These objective assessment findings agree with the visual assessment.

Considering IQA from various comprehensive assessment standards the best overall reconstruction

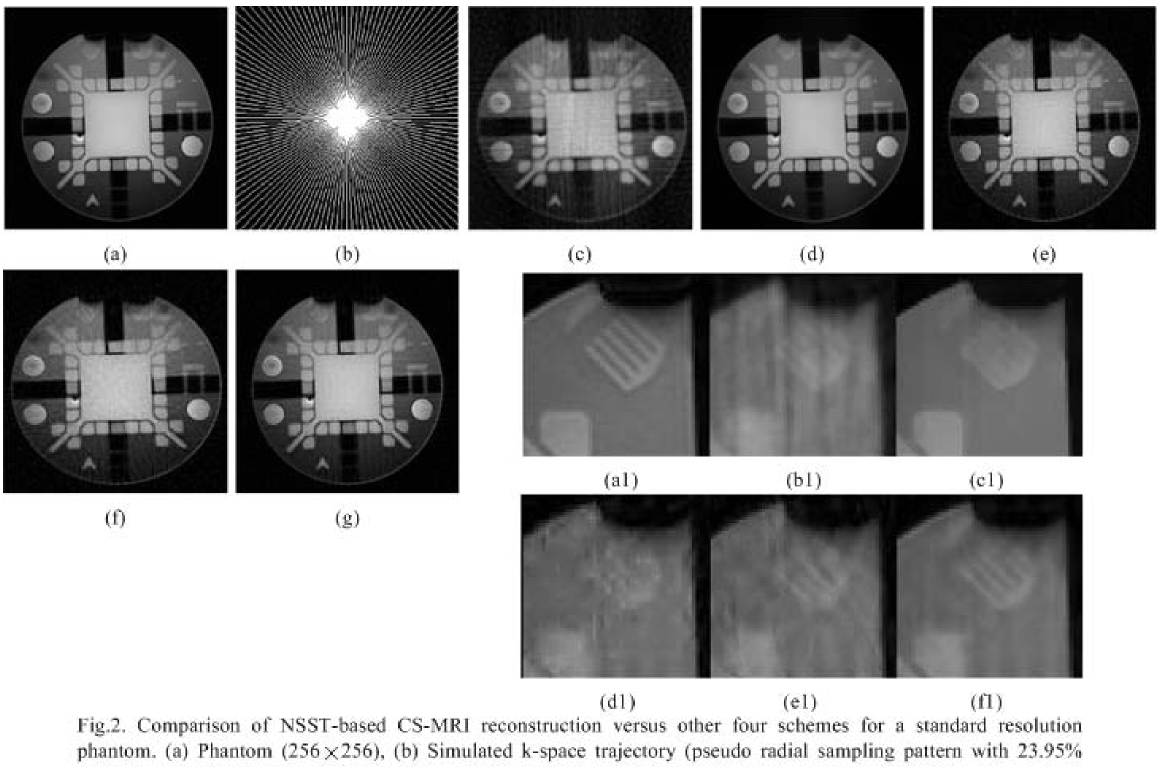

Fig.2. Comparison of NSST-based CS-MRI reconstruction versus other four schemes for a standard resolution phantom. (a) Phantom (256×256), (b) Simulated k-space trajectory (pseudo radial sampling pattern with 23.95% sampling rate),(c)~(g) Reconstruction using zero-filling, TV-CG, ODWT-based, SFLCT-based and the proposed NSST-based CS-MRI, respectively, (a1)~(f1) Enlargements of (a), (c)~(g) for acertain region.

performance is achieved by the proposed NSST-based CS-MRI reconstruction method. Its performance is superior to other comparing algorithm. Furthermore, it has good stability of MR images reconstruction.

V. Conclusion

In this paper, a novel CS-MRI reconstruction based on NSST sparsity prior is proposed. NSST is an excellent multi-resolution geometric analysis tool which possesses optimal approximation property and provides an optimal sparse representation in terms of better spatial localization, highly directional sensitivity, and anisotropy and shift invariance. More intrinsic information can be preserved in reconstructed MR image with improved visual quality. Numerical experiments demonstrate that CS-MRI reconstruction using NSST shows better performance compared with other methods. The subjective visual and the comparisons of objective evaluation indices all demonstrate that our proposed method can preserve more details of MR image, and can greatly improve visual quality of reconstruction image with much less graininess and less information distortion than the others. Efficient implementation of the proposed method, e.g. by using the computation power of Graphics Processing Unit is expected. Moreover, the application of some adaptive sparse representations would be explored in a future work.

Acknowledgment

This work was partially supported by National Natural Science Foundation of China (No.61175012 & 61201422), Specialized Research Fund for the Doctoral Program of Higher Education of China (No. 2011021111-0026), and the Fundamental Research Funds for the Central Universities of China (No.lzujbky-2010-220, No.lzujbky-2012-38, No. lzujbky-2013-k06, No. lzujbky-2013-41). The authors would like to thank Dr M. Lustig for sharing the interface framework of CS-MRI, Dr Demetrio Labate for sharing the Shearlet Toolbox and Dr Xiaobo Qu for sharing some demos. The authors also would like to thank American Radiology Services (http://www3.americanradiology.com/pls/web1/wwimggal.vmg/) to provide valuable medical images.

References

[1] D. L. Donoho, "Compressed sensing," *Information Theory, IEEE Transaction on,* vol.52, no.4, pp.1289–1306, 2006.
[2] E. J. Candès, J. Romberg, and T. Tao, "Robust uncertainty principles: exact signal reconstruction from highly incomplete frequency information," *Information Theory, IEEE Transaction on*, vol.52, no.2, pp.489–509, 2006.
[3] Y. Tsaig, and D. L. Donoho, "Extensions of compressed sensing," *Signal Processing*, vol.86, no.3, pp.549–571, 2006.
[4] M. Lustig, D. Donoho, and J. M. Pauly, "Sparse MRI: the application of compressed sensing for rapid MR imaging," *Magnetic Resonance in Medicine*, vol. 58, no. 6, pp. 1182–1195, 2007.
[5] J. Trzasko, and A. Manduca, "Highly undersampled magnetic resonance image reconstruction via homotopic l_0-minimization." *Medical imaging, IEEE Transaction on,* vol.28, no.1, pp. 106-121, 2009.
[6] J. P. Haldar, D. Hernando, and Z. Liang, "Compressed-sensing MRI with random encoding," *Medical Imaging, IEEE Transaction on*, vol.30, no.4, pp.893-903, 2011.
[7] K. T. Block, M. Uecker, and J. Frahm. "Undersampled radial MRI with multiple coils. Iterative image reconstruction using a total variation constraint," *Magnetic resonance in medicine*, vol.57, no.6, pp.1086-1098, 2007.
[8] J. Huang, S. Zhang, D. Metaxas, "Efficient MR image reconstruction for compressed MR imaging," *Medical Image Analysis*, vol. 15, no. 5, pp. 670-679, 2011.
[9] M. N. Do and M. Vetterli, "The contourlet transform: An efficient directional multiresolution image representation," *Image Processing, IEEE Transaction on*, vol.14, pp.2091–2106, 2005.
[10] S. M. Gho, Y. Nam, S. Y. Zho, E. Y. Kim, and D. H. Kim, "Three dimension double inversion recovery gray matter imaging using compressed sensing," *Magnetic resonance imaging*, vol.28, no.10, pp.1395-1402, 2010.
[11] Y. Lu, M. N. Do, "A new contourlet transform with sharp frequency localization," *in Proceeding of IEEE International Conference on Image Processing,* 2006, pp. 1629-1632.
[12] X. Qu, W. Zhang, D. Guo, C. Cai, S. Cai, and Z. Chen. "Iterative thresholding compressed sensing MRI based on contourlet transform," *Inverse Problems in Science and Engineering*, vol.18, no.6, pp.737–758, 2010.
[13] N. G. Kingsbury, "The dual tree complex wavelet transform: a new efficient tool for image restoration and enhancement," *in Proceedings of the European Signal Processing Conference*, pp.319–322, 1998.
[14]Y. Kim, M. Altbach, T. Trouard, and A. Bilgin, "Compressed sensing using dual-tree complex wavelet transform," *in Proceedings of the International Society for Magnetic Resonance in Medicine*, vol. 17, pp. 2814, 2009.
[15] Z. Zhu, K. Wahid, P. Babyn, and R. Yang, "Compressed sensing-based MRI reconstruction using complex double-density dual-tree DWT," *Journal of Biomedical Imaging*, vol.2013, 2013.
[16] Y. Kim, M. S. Nadar, and A. Bilgin. "Wavelet-based compressed sensing using gaussian scale mixtures," *in Proc. Intl. Soc. Mag. Reson. Med. 18,* pp.4856, 2010.
[17] Y. Kim, M. S. Nadar, and A. Bilgin. "Wavelet-based compressed sensing using a Gaussian scale mixture model," *Image Processing, IEEE Transaction on*, vol.21, no.6, pp.3102-3108, 2012.
[18] C. Chen, J. Huang, "Compressive Sensing MRI with Wavelet Tree Sparsity," *in Proc. of the 26th Annual Conference on Neural Information Processing Systems (NIPS)*, Nevada, USA, Dec.2012.
[19] C. Chen, J. Huang. "The benefit of tree sparsity in accelerated MRI," *Medical Image Analysis*, vol.18, no.6, pp. 834–842, 2014.
[20] S. Ma, W. Yin, Y. Zhang, and A. Chakraborty, "An efficient algorithm for compressed MR imaging using total variation and wavelets," *in Proceedings of the 26th IEEE Conference on Computer Vision and Pattern Recognition (CVPR '08)*, June 2008.
[21] J. Huang, Yang F., "Compressed magnetic resonance imaging based on wavelet sparsity and nonlocal total variation," *in the 9th IEEE International Symposium on Biomedical Imaging (ISBI)*, Bacelona, Spain, pp.968-971, 2012.
[22] X. Qu, X. Cao, D. Guo, C. Hu, and Z.Chen, "Combined sparsifying transforms for compressed sensing MRI," *Electronics letters*, vol.46, no.2, pp.121-123,2010.
[23] C. Chen, J. Huang and L. Axel, "Accelerated Parallel Magnetic Resonance Imaging with Joint Gradient and Wavelet Sparsity," *MICCAI Workshop on Sparsity Techniques in Medical Imaging*, Nice, France, Oct 2012.
[24] S. Ravishankar, B. Yoram, "MR image reconstruction from highly undersampled k-space data by dictionary learning," *IEEE Transaction on Medical Imaging,* vol.30, no.5, pp.1028-1041, 2011.
[25] G. Easley, D. Labate, W. Q. Lim, "Sparse directional image representations using the discrete shearlet transform," *Applied and Computational Harmonic Analysis*, vol.25, no.1, pp. 25-46, 2008.
[26] D. Labate, W.Q. Lim, G. Kutyniok, and G. Weiss, "Sparse multidimensional representation using shearlets," *in Proc. SPIE Wavelets XI,* San Diego, CA, vol. 5914, pp. 254–262,2005.
[27] Lim W.Q., "The discrete shearlet transform: A new directional transform and compactly supported shearlet frames," *IEEE Transaction on Image Processing*, vol.19, no.5, pp.1166-1180, 2010.
[28] G. Kutyniok, W. Q. Lim, and X. Zhuang, "Digital Shearlet Transforms," *Shearlets*. Birkhäuser Boston, pp. 239-282, 2012.
[29] I. Daubechies, M. Defriese, and C. De Mol, "An iterative thresholding algorithm for linear inverse problems with a sparsity constraint," *Communications on Pure and Applied Mathematics*, vol.57, no.11, pp.1413-1457, 2004.
[30] M. Figueiredo, R. Nowak, "An EM algorithm for wavelet-based image restoration," *IEEE Transaction on Image Processing*, vol.12, no.8, pp.906-916, 2003.
[31] K. Bredies and D. A. Lorenz, "Linear convergence of iterative soft-thresholding," *Journal of Fourier Analysis and Applications,* vol.14, pp. 813–837, 2008.
[32] I. Drori, "Fast l1 minimization by iterative thresholding for multidimensional NMR spectroscopy," *EURASIP Journal on Advances in Signal Processing 2007,* vol.2007.
[33] M. Zibulevsky, M.Elad, "L1-L2 Optimization in signal and image processing," *IEEE Signal Processing Magazine,* vol.27, pp.76-88, 2010.
[34] W. Yin, S. Osher, D. Goldfarb, "Bregman iterative algorithms for l1-minimization with applications to compressed sensing," *SIAM Journal on Imaging Sciences*, vol.1, no.1, pp.143-168, 2008.
[35] Z. Wang, A. C. Bovik, H. R. Sheikh and E. P. Simoncelli,"Image quality assessment: From error visibility to structural similarity,"*IEEE Transactions on Image Processing*, vol. 13, no. 4, pp. 600-612, 2004.
[36] C. S. Xydeas, V. Petrovic, "Objective image fusion performance measure," *Electronics Letters*, vol.36, no.4, pp.308–309, 2000.

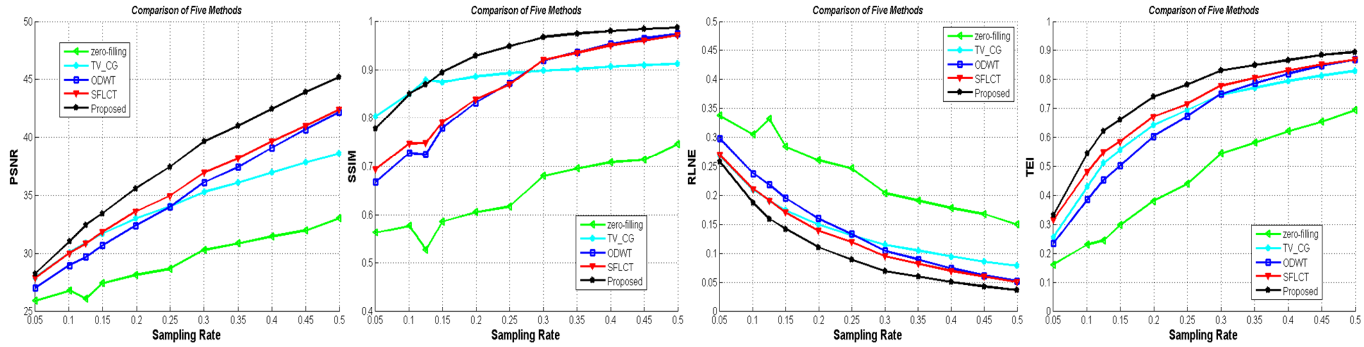

(a) (b) (c) (d)

Fig.3. Objective assessment indices of five schemes. (a)~(d) PSNR, SSIM, RLNE and TEI versus undersampling rate, respectively.